The Synthesis and Characterization of Ni-W-C Alloy Powders by H_2-CH_4 Reaction with Oxides

Michał Mis[1], Neha Sardana[2], Seshadri Seetharaman[3,*]

[1]*Faculty of Non-Ferrous Metals, AGH - University of Science and Technology, Kraków, Poland,*
[2]*Metallurgical & Materials Science Department, Indian Institute of Technology Roorkee, India,*
[3]*Department of Materials Science and Engineering, Royal Institute of Technology (KTH), Stockholm, Sweden*

(Received November 7, 2008 ; final form December 14, 2008)

ABSTRACT

With a view to developing a more energy-efficient and environment-friendly process route for the production of W-C based cutting tools, a single step process for the synthesis of tungsten carbides containing Ni from oxide precursors was investigated in the present work. A fluidized bed reactor was employed, wherein the mixed oxides were subjected to simultaneous reduction and carburization using H_2-CH_4-Ar gas mixtures in the temperature range 1073-1273 K. The carbon potential in the gas phase could be accurately controlled by suitably adjusting the H_2/CH_4 ratio. The impact of gas flow rates and temperature on the reaction product was examined. The carbide product obtained was characterized by SEM and X-ray diffraction. The results showed that the product consisted of Ni-W-C alloys, which were in consistency with the phase diagram at the temperature of reaction. The particle size of the carbides is in the range of 10^{-8}m, which was dependent on the process temperature, higher temperature yielding larger grains. The results indicate that the gas-solid reaction route combining reduction and carburization is an efficient method that can be commercially applied for the production of a variety of cemented carbides.

Keywords: alloy, powder metallurgy, carburization, tungsten carbide,

1. INTRODUCTION

Cemented carbides have been known for a long time as suitable materials for cutting tools, due to their high hardness and toughness /1/. These are often composites containing Ti/W-C+Ni/Co/Cr/Fe. These carbides have distinct microstructure and superior physical properties; but work is still being carried out for the increase in high-temperature strength, chemical stability and oxidation resistance /2/ in order to increase their application towards metal forming, mining and construction tool industries.

It is known that the toughness of cemented carbide composites decreases with the increase of hardness. But as the grain sizes are reduced from the macro to micro/nano level, both the toughness and hardness increase /3/. Hence, efforts are made in order to reduce the grain sizes of cemented carbides to nano levels to get better hardness with simultaneous increase in toughness. Many methods for the production of such carbides with improved properties have been investigated. These are mostly based on the powder metallurgy route, which is a challenge in itself to reduce the grain size to nano levels.

Another challenge faced by this industry is to produce the cemented carbides by means of a cost effective and environmentally friendly process. Traditionally the powdered materials Ti/W-C were physically mixed with Co/Ni/Cr/Fe. However, in recent

* Corresponding author: e-mail address: raman@kth.se, tel: +46-8-790 83 55, fax: +46-8-790 09 39

years, sophisticated and precise methods as, for example, chemical processing by the spray conversion, are increasingly being introduced for the synthesis of cemented carbides.

In the present work, a simultaneous reduction-carburization of the oxide precursors for the cemented carbides was carried out in a fluidized bed reactor. A number of earlier studies in the present laboratory on the hydrogen reduction of oxides have shown that this gas-solid reaction route is an environmentally friendly single step process towards the production of alloys /4/, intermetallics /5/ and composite materials /6/ with product uniformity even in a nanoscale. The present work is an extension of this process concept towards simultaneous reduction-carburization method for the production of cemented carbides from the oxides. This is enabled by the use of H_2-CH_4 mixtures that can effectively fix the carbon potential in the gas phase. The present concept has the advantage that this is a single step process. A perfect fluidized bed provides nascent metal particles (Ni, W) with free C in the vicinity inside the reactor. These reactive particles could easily combine among themselves to form a uniform carbide composite. The carbon potential could easily be controlled by varying the H_2-CH_4 ratio as well as reaction temperature. The latter also has a strong impact on the grain size of the product. Such a process route has the advantage that no environmentally undesirable gas product is produced.

1.1 Previous Work on Ni-W-C Synthesis

A survey of the previous work published reveals that the WO_3 reduction with CO-CO_2 mixtures was produced in a single step process in 1986 /7/ to give WC in the temperature interval 973-1373K. The nucleation and growth of the product were dependent on the temperature of the reaction. At higher temperatures, the reaction rate was governed by the reduction of WO_2 to W with the intermediates as $W_{20}O_{58}$, $W_{18}O_{49}$, WO_2 and W /7/. Further in 1995, a similar WO_3 reduction with CO came into consideration with the thermo-gravimetric study from 923 to 1173K with the final product as WC and the above-mentioned intermediate phases. The energies of activation were calculated as 40 and 62 kJ mol^{-1} for reduction of WO_3 and WO_2 respectively /8/.

A successful reduction with CH_4-H_2-Ar gas mixture was carried out in Australia /9/, for reduction and carburization of the oxides of iron, manganese, chromium, and titanium, in a fixed-bed reactor in temperature-programmed and isothermal-reduction experiments. It was observed that methane-containing gas with high carbon activity provided strongly reducing conditions, in which metal oxides were reduced and carburized to metal carbides /9/. The summary of the above is shown in **Table 1**.

Table 1

Previous work conducted on the reduction-carburization of oxides

Oxides of	Intermediates:	Final product
Iron	Fe	Fe_3C
Manganese	-	Mn_7C_3
Chromium	-	Cr_3C
Titanium	TiO_2, Ti_5O_9, Ti_4O_7, Ti_3O_5, Ti_2O_3	TiO_xC_v
*Tungsten	$W_{20}O_{58}$, $W_{18}O_{49}$, WO_2, (WC_2)	WC
The carburization- reduction was carried with the gas mixture CH_4-H_2-Ar /9/, * only CO was used /8/.		

It was also seen that the reduction by methane-containing gas occurs through adsorption and dissociation of methane with the formation of adsorbed active carbon. Deposition of solid carbon during the process was found to retard the reduction. /9/

In a method proposed by Inframat Corporation /10/, the ultrafine precursors W and C are produced via a wet chemical process, followed by continuous heat-treatment schedule at controlled stages leading to highly fine and structured WC material. The as-synthesized WC powder has an average grain size of ~ 40 nm /10/. These nanograined WC particles are agglomerated resulting in an average agglomerate size of 0.2 to 0.4 micron /10/. Fine-grained WC/Co-Ni composite could be synthesized by an addition of Co/Ni source into the WC materials.

2. EXPERIMENTAL METHOD

2.1. Materials

NiO supplied by Sigma-Aldrich Sweden AB, (99% purity, 325 mesh); and WO_3 supplied by Atlantic Equipment Engineers (99.9% purity 1-5 microns grain size) were used in the synthesis of Ni-W-C composites in the present work. Hydrogen gas (Scientific, OTC-50), methane (Chemical, OTC-10) and argon (ICP 5.0) were supplied by AGA Gas AB, Stockholm.

Great care was taken to purify the gases used in the fluidized bed reactor. The hydrogen gas was passed through Pt catalyst so that the oxygen impurity in the gas could react with hydrogen forming H_2O. The gas was then passed through columns of silica gel and $Mg(ClO_4)_2$, to dry the gas to extremely low moisture levels. The methane gas used was dried in a similar way. The argon gas was dried using columns of silica gel and $Mg(ClO_4)_2$. The CO_2 impurity in the gas was removed by passing the gas through a column of Ascarite. The traces of oxygen in the gas were removed by first passing the gas through a column of copper turnings (maintained at 973K) and then through a column of Mg tunings (maintained at 773 K). The argon gas thus purified was found in earlier studies in the present laboratory, to have an oxygen pressure lower than 10^{-14} Pa. This precaution is essential in order to ensure that the fine-grained reaction product, which is extremely reactive, is not reoxidized in argon atmosphere during cooling, after the reduction-carburization treatment. All the gases were mixed in a gas mixer chamber filled with glass beads, before entering the fluidized bed reactor.

2.2. The apparatus

Vertical fluidized bed reactor used in the present experimental work was fabricated at Webelco, Spånga, Sweden. The reactor tube consists of a glass tube of 15 mm inner diameter, 18 mm outer diameter and 1000 mm long with a porous quartz disc fused at the centre of the tube. The average pore size of the disc was 200μm. The reactor tube was positioned in a vertical furnace with Kanthal A-1 heating element, capable of reaching a maximum temperature of 1523 K. The furnace has an even temperature zone of 100 mm. The reactor tube was mounted in such a way that the porous disc was at a level of about 20 mm. below the centre of the even temperature zone of the furnace. The temperature of the fluidized bed was measured by a K-type thermocouple.

2.3. Procedure

The oxide precursors, *viz.* NiO and WO_3 were accurately weighed and mixed in the ratio of 8.56 mass % NiO and 91.44 mass % WO_3. The oxide mixture was finely ground in an agate mortar, ensuring thorough mixing. About 2 g of the powder mixture was introduced into the reactor. The reactor was purged with argon gas, at a flow rate 0.2 l/min till the targeted experimental temperature was reached. The Ar flow was then decreased to 0.1 l/min and H_2–CH_4 mixture was introduced so that the total gas flow was kept as 0.2 l/min (the linear velocity was above the range of the value for fluidization for the present reactor, *viz.*0.025-0.035 mm/s). The final gas mixture introduced into the system always had 50 vol % of argon, which diluted the gas mixture to attain the targeted C-potential.

The reduction-carburization experiments were conducted under isothermal conditions. Preliminary experiments showed that the reduction was very slow below 973 K (the minimum temperature in the present series). One sample, "STT" was synthesized at 973K and with a CH_4 content of 5 vol %. In this sample, stable phase of nickel and two phases of tungsten carbide – WC and W_2C were observed. These observations are in agreement with the earlier work by Löfberg *et al.* /11/. Above 1273 K as the reaction temperature, the grain growth in the product was significant. Thus the temperature range of the synthesis in the present investigation was restricted to 1073 – 1273 K.

All the experiments were carried out for a period of 4 hrs which was determined in preliminary experiments as the time required for complete reduction at the lowest reaction temperature in the present series /12-16/. The hydrogen to methane ratio and the temperatures considered in our experimentation are listed in **Table 2.**

Table 2
Reaction conditions for all samples

Gas mixture: 50 vol % Ar		Temperature [K]		
CH_4[vol %]	H_2[vol %]	1073	1173	1273
5	45	S01	S02	S03
10	40	S04		S05
15	35	S06	S07	S08
20	30	S09		

After the reduction, the samples were furnace-cooled in argon atmosphere and stored in a desiccator. The samples were characterized by XRD and SEM analyses. For the XRD analysis, a Siemens D5000 X-Ray Diffractometer unit (with the software used for XRD analysis, DIFFRAC plus XRD Commander and EVA2 by SOCABIM) was used. SEM observations of most samples were performed using JEOL JSM-840 with an EDS Link AN 10000 scanning microprobe. Two samples were investigated using high resolution SEM with scanning microprobe (Nova 600 Nano-Lab Dual Beam-SEM/FIB manufactured by FEI Company). All the samples were investigated for W and Ni contents. Additionally, some samples were examined for impurities such as oxygen, iron and silicon. The bulk carbon analysis was carried out by LECO combustion method.

Grain size was measured using straight-line method. Due to large grain size variations, grain size measurements were considered to be associated with large uncertainties.

3. RESULTS

The results obtained in the present investigation comprise of bulk carbon analysis, XRD and SEM-EDS analyses including the high resolution SEM analysis. As mentioned earlier, the grain size was estimated from the SEM images. The chemical composition of individual grains was obtained by EDS analysis.

3.1. Bulk carbon analysis results

The determination of the bulk carbon was carried out with two samples from the same batch and the results are in agreement. Bulk carbon analysis results are presented in **Table 3**. The carbon content is found to vary from 9.6 mass % to 15 mass % (except in the case of sample S09 where a very high C-content, 23.85 mass % was noticed). This increase in the carbon content can be seen as related to the amount of CH_4 in the gas phase, which increases the carbon potential.

Table 3
Bulk carbon analysis results

Sample [ID]	Measurement 1 [mass %]	Measurement 2 [mass %]	Average [mass%]
S01	9.67	9.71	9.69
S02	11.20	11.40	11.30
S03	9.99	10.00	10.00
S04	11.80	12.00	11.90
S05	13.70	13.80	13.75
S06	14.90	15.20	15.05
S07	11.30	11.30	11.30
S08	9.66	9.69	9.68
S09	23.70	24.00	23.85

3.2. XRD analysis results

All the samples synthesized were subjected to XRD analysis. Most of the XRD patters of samples S01 – S08 were quite similar showing the presence of WC and Ni phases. The pattern corresponding to the sample S01 is shown in **Figure 1**.

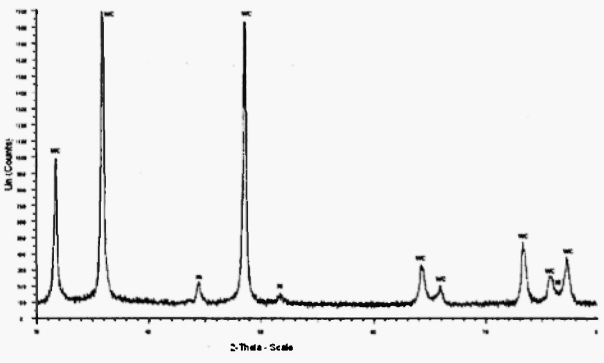

Fig. 1: XRD pattern of S01

Only pure WC and Ni reference peaks could be fitted to the XRD patterns obtained for these samples.

No other peaks were found. In the case of sample S09, which was synthesized at high CH_4 content in the gas phase, the XRD analysis indicated the presence of free carbon, (**Figure 2**). This is in conformity with the bulk carbon analysis of this sample.

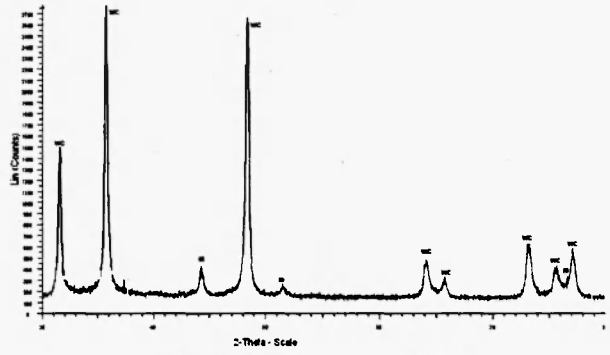

Fig. 2: XRD pattern of S09

A summary of the phases present in all the samples obtained by XRD analysis is presented in **Table 4**.

Table 4
XRD results with temperatures and CH_4 content in the gas phase

Sample ID	Temperature [K]	CH_4 [vol %]	WC	Ni	W	C	NiO	WO
S00	N/A	N/A					X	X
S01	1073	5	X	X				
S02	1173	5	X	X				
S03	1273	5	X	X				
S04	1073	10	X	X				
S05	1273	10	X	X				
S06	1073	15	X	X				
S07	1173	15	X	X				
S08	1273	15	X	X				
S09	1073	20	X	X		X		

Presence of substance is indicated by X

3.3. SEM-EDS and High Resolution SEM Analysis results:

All the samples listed in Table 1 were subjected to SEM-EDS analysis. High resolution EDS results were obtained for samples S04 and S06. These results are presented in **Table 5**.

S00 sample was the source powder. The sample was examined using SEM. The SEM image is presented in **Figure 3**. The grain size was found to vary between 0.4μm and 2.5μm and the grains were of irregular shape as can be seen in the figure. The mean intersection length was 0.73μm. XRD of NiO-WO_3 sample indicated the presence of only NiO and WO_3 in this sample.

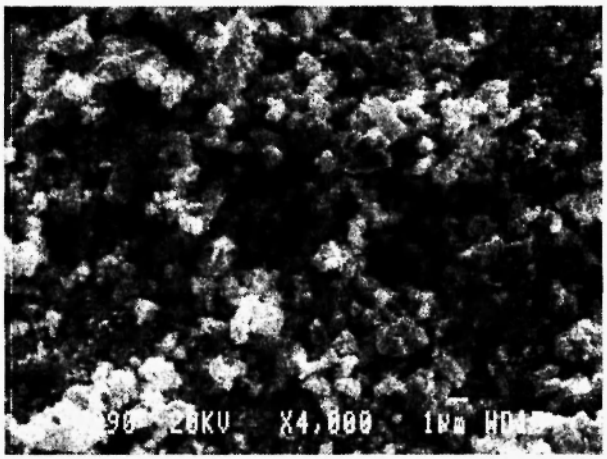

Fig. 3: SEM image of S00, magnification 4000X

Figure 4 presents the SEM image of the sample S01 reduced at 1073K with the highest H_2/CH_4 ratio. SEM images clearly showed the presence of agglomerates of small particles. Each small particle had varying shapes ranging from spherical to elongated, the size of smallest grain being 0.2μm to 0.4μm. The agglomerate size was generally found to be about 2μm, and mean intercept length, 0.58μm.

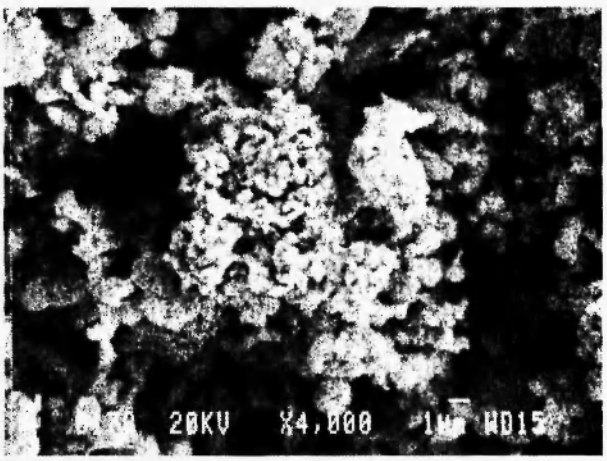

Fig. 4: SEM image of S01, magnification 4000X

Table 5
Results of high resolution EDS without line scan

Sample ID	Site	Spectrum	B [mass %]	C [mass %]	O [mass %]	Ni [mass %]	Zr [mass %]	W [mass %]
S04	Site of interest 1	Spectrum 1	0	59.14	0	3	0	37.86
		Spectrum 2	0	35.87	0	0	0	64.13
		Spectrum 3	0	5.21	0.49	1.3	0	93
		Spectrum 4	0	73.33	4.18	14.93	7.56	0
		Spectrum 5	2.53	30.55	0	2.73	54.28	0
		Max	2.53	73.33	4.18	14.93	54.28	93
		Min	0	5.21	0	0	0	0
		Mean	0.506	40.82	0.934	4.392	12.368	38.99
	Site of interest 2	Spectrum 1	0	24.8	0	7.97	0	67.23
		Spectrum 2	0	78.93	0.92	4.63	0	15.53
		Spectrum 3	0	76.89	1.52	6.45	0	15.02
		Spectrum 4	0	74.45	0.89	5.85	0	18.8
		Spectrum 5	0	99.12	0.88	0	0	0
		Max.	0	99.12	1.52	7.97	0	67.23
		Min.	0	24.8	0	0	0	0
		Mean	0	70.83	0.842	4.98	0	23.31
S06	Site of interest 1	Spectrum 2	0	26.12	0	1.97	0	71.91
		Spectrum 3	0	25.36	0	0	0	74.64
		Spectrum 4	0	26.89	0	1.54	0	71.58
		Spectrum 5	0	30.2	0	2.15	0	67.65
		Max.	0	30.2	0	2.15	0	74.64
		Min.	0	25.36	0	0	0	67.65
		Mean	0	27.14	0	1.415	0	71.44
	Site of intrest 2	Spectrum 1	0	24.15	0	1.55	0	74.31
		Spectrum 2	0	18.23	0	1.83	0	79.94
		Max.	0	24.15	0	1.83	0	79.94
		Min.	0	18.23	0	1.55	0	74.31
		Mean	0	21.19	0	1.69	0	77.12

Figure 5 shows the SEM image of sample S04 prepared using 10 vol % methane at 1273 K. The SEM image shows very small round particles and big elongated or shapeless particles. Grain size was found to vary in a broad range, mean intersection length being 0.61μm.

High resolution SEM was performed for this sample in three places.

The images obtained, which are presented in **Figures** 6 and 7, show that each bigger grain consists of many smaller particles; each particle is bound together with a number of other particles. Shattered edges of particles are, in fact, smaller particles that are located on the surface of the agglomerate. Small particles are of size under 0.1μm and small particle size varies.

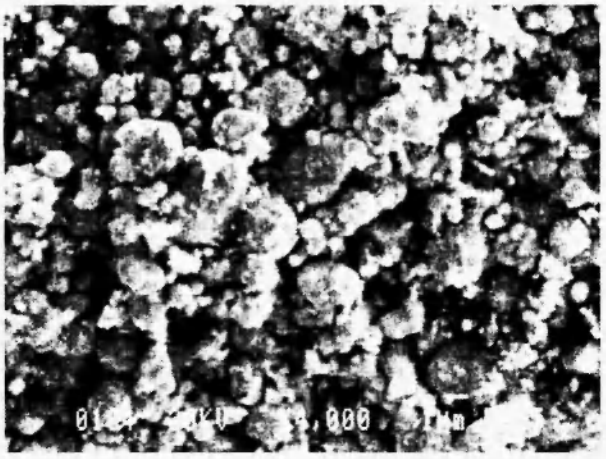

Fig. 5: SEM image of S04, magnification 4000X

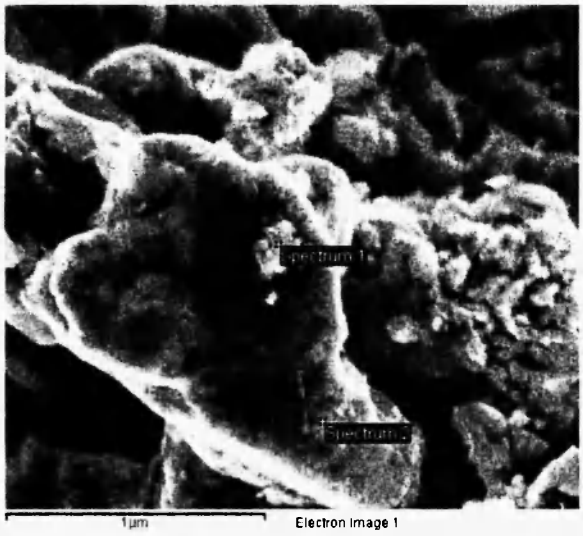

Fig. 6: High resolution SEM for S04

At the center of Figure 6, a shapeless, big grain over 6µm length is seen. This grain has curved texture suggesting that it is a big agglomerate of smaller particles. In the left bottom and left central part, thread like, bright structures are seen. There are also very dark particles d = ca 1.3µm. EDS investigation of this site was performed at 5 points. In all points, different compositions of the grain were detected. Generally, there is more carbon than expected from bulk carbon analysis or XRD test.

The various sites of interest, shown in Figure 6, identified in the SEM images provide interesting structure information. At site 2, one big grain and some smaller are seen. EDS indicates that big grain consists of carbon and very small amount of oxygen. The grain is 1.1µm diameter, round shaped. On the left side of the grain, the texture seen suggests that the big grain is an agglomerate of smaller grains, d = circa 0.2 µm. There is also a thread like structure seen that consists mostly of carbon and some nickel and tungsten. The thread like structure is 1.1µm long. Spectrum 4 indicates 74.45 mass % of carbon, 0.89 mass % of oxygen, 5.85 mass % of nickel and 18.8 mass % of tungsten in bright grain.

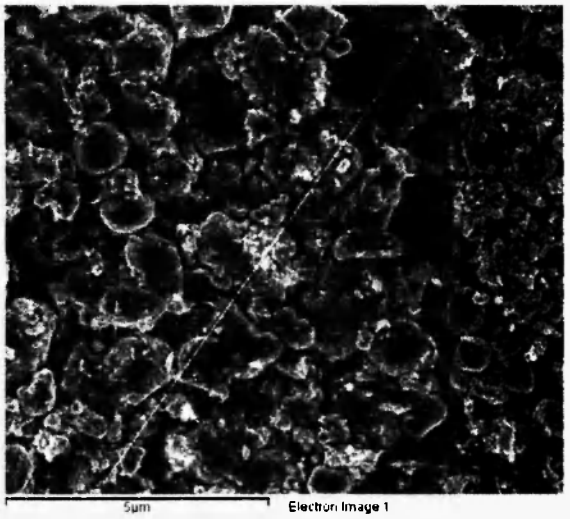

Fig. 7: High resolution SEM of S04 with indicated line scan

A line scan area of this sample is presented in **Figures 7a** and **7b**. On this image, one can see various grain sizes. Grains are generally equiaxial, elongated and shapeless with shattered edges. The shape of the smallest grain is elongated and creates a thread like structure visible in various points. Some small grains are very bright and round shaped. Bigger grains are more irregular in shape (probably indicating more shattered surface). A line scan of this sample is represented in **Figure 8**. Sample composition varies along this line. The big grain at upper end of line consists mostly of carbon. It can also be seen that relatively nickel-rich grains are present in this sample.

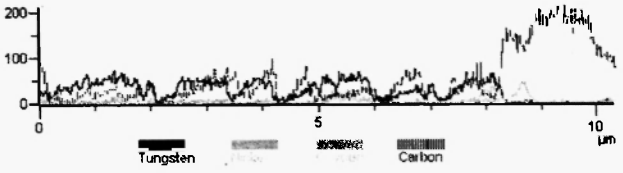

Fig. 8: Line scan of S04

S06 sample was treated at 1073 K in an atmosphere containing 15 vol % methane. The corresponding SEM image (**Figure 9**) shows the presence of various grain sizes and shapes, smallest grain being under 0.5μm and the biggest about 2μm. EDS investigation detected only carbon, nickel and tungsten. Average amount of carbon is 27.14 mass %, nickel is 1.45 mass % and tungsten is 71.44 mass %.

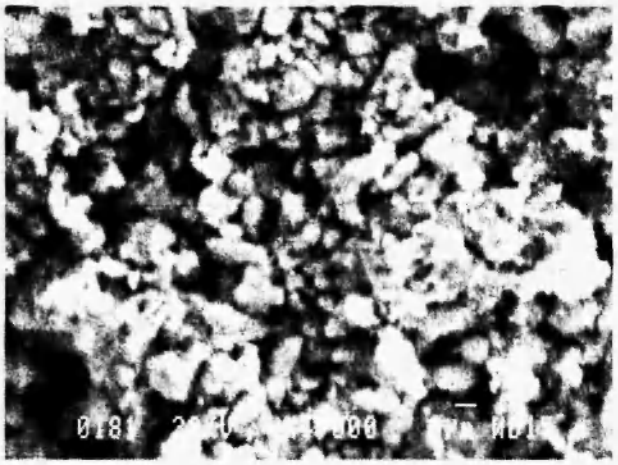

Fig. 9: SEM image of S06, magnification 4000X

Figure 10 shows the high resolution SEM image obtained for the sample S06. One grain consists almost only of carbon. In the second scan, Figure 11, one very big grain can be seen in the center of picture and smaller grains around it. At the left bottom, a thread like structure is seen. This area also contains very small, bright particles. There are some points rich with nickel. Every big grain on this image has a shattered surface and it can, in fact be deduced that it is an agglomerate of smaller grains. It is possible to see very small particles on the surface of big grains and between them, which actually gives the real grain size of the powder.

A line scan was performed on this sample and the site is shown in **Figure 11.** This line goes through one big grain. The composition analysis is presented in **Figure 12.** It is seen that the composition is fairly uniform along the line examined confirming the potential of the method to produce uniform samples. One anomalous result was found at the position, where the carbon content is quite high while the corresponding tungsten content is very low.

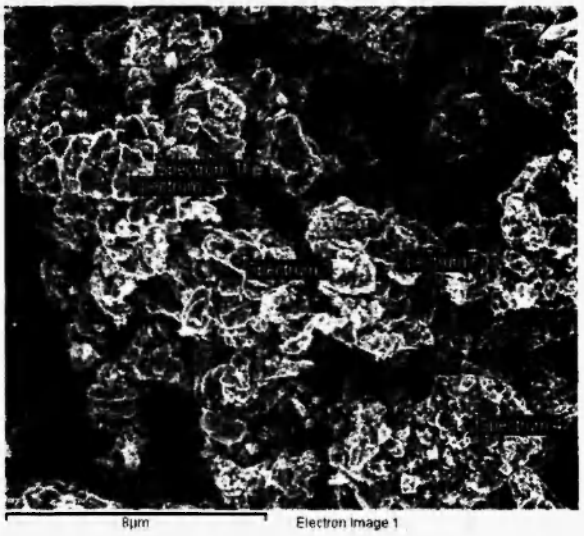

Fig. 10: High resolution SEM for S06

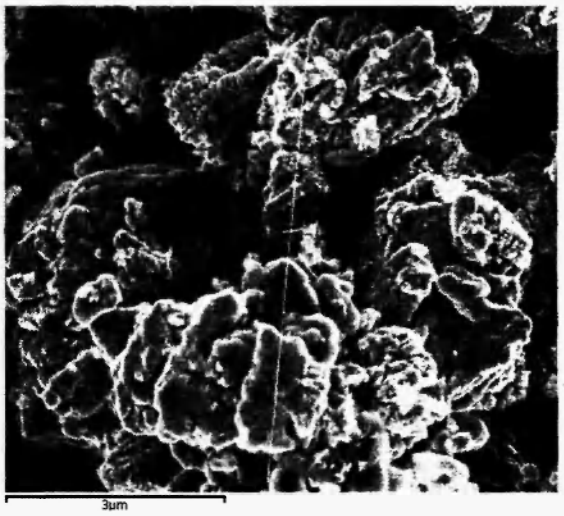

Fig. 11: High resolution SEM image of S06 with indicated EDS scan line

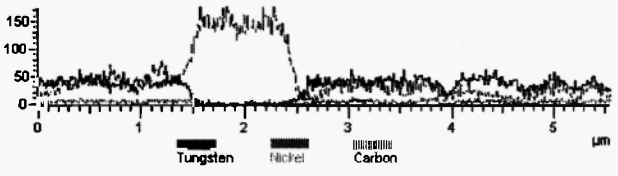

Fig. 12: Line scan of S06

It is interesting to note that the results of high resolution EDS indicate the presence of C nano particles.

Table 6
Low resolution EDS results

Sample ID	Ni cont. [mass%]	W cont. [mass%]	O cont. [mass%]	Si cont. [mass%]	Fe cont. [mass%]
S00	9.51	63.23			
	9.62	61.38	27.45	1.41	0.14
S01	17.42	82.56			
	16.90	75.34	5.00	2.76	
	16.47	83.53			
S02	10.02	89.98			
	10.19	89.81			
S03	32.76	67.24			
	11.13	88.87			
	15.32	84.68			
S04	8.90	91.10			
	6.96	93.04			
S05	12.07	84.13	3.80		
	13.21	82.77	4.02		
S06	13.90	86.81			
	14.25	85.75			
S07	7.91	92.09			
	11.75	88.25			
S08	9.34	90.66			
	8.45	78.17	10.28	2.26	0.84
	8.68	91.32			
	8.05	79.79	9.41	2.70	0.05
S09	12.75	87.25			
	11.74	75.88		2.54	0.41

The EDS results of all the samples from the low resolution SEM images are presented in **Table** 6. In the case of the samples S01 – S06, the Ni content is found to vary between 9 and 16 mass % (except one point in the case of sample S03, where the Ni-content was as high as 32.76 mass % which is anomalous). Similarly, the tungsten content is found to vary within the band 61 mass % and 93 mass %. The variations are attributed to the different H_2/CH_4 ratios used for the synthesis of these samples. The oxygen detected could be due to the surface oxidation of the product. In any case, oxygen contents by EDS analysis were considered unreliable. Si impurities may have been caused by use of Agate mortar.

Table 7
Grain size together with reaction temperature

Sample ID	Temperature [K]	Grain size [μm]
S00	n/a	0.73
S01	1073	0.58
S02	1173	0.66
S03	1273	0.65
S04	1073	0.61
S05	1273	0.78
S06	1073	0.76
S07	1173	0.65
S08	1273	0.85
S09	1073	0.62

Table 7 shows the grain sizes obtained for the various samples synthesized at different temperatures. It is seen that the grain size increases with the temperature of synthesis.

4. DISCUSSION

The targeted composition for the cemented carbide in the Ni-W-C system is 10 mass % Ni and 90 mass % WC (5.51 mass % C and 84.49 mass % W). The ternary phase diagram for the Ni-W-C system at 1073 K, obtained from the thermochemical database, THERMOCALC /17/, is presented in **Figure 13**.

The targeted composition is marked in the figure with the black dot. It is seen that this composition lies on the WC-Ni tie line. The XRD results from the present work at 1073 K show that the phases present in the product are WC and Ni, in conformity with the phase diagram. The average compositions of these samples from Table 6 can be combined with bulk carbon contents in Table 3 to get the total compositions of the samples, normalized to 100 mass % (corresponding to 1073 K). Normalized compositions of samples are presented in **Table 8**. These compositions are also plotted in Figure 13. It is seen that the compositions of the samples are slightly moved towards pure carbon lying in the three phase area Ni (FCC) -WC - C. Since the amount of free carbon in samples S01, S04 and S06 are relatively low; the corresponding XRD peaks may not be detected in the XRD spectrum. In the case of sample S09 with high carbon content, the sample composition has moved further towards C corner.

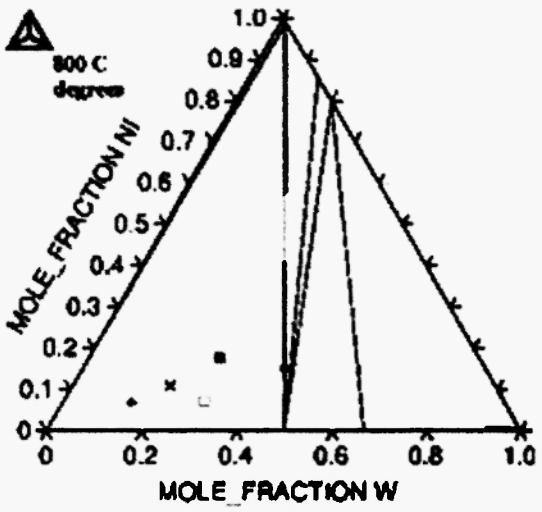

Fig. 13: The isothermal section of the Ni-W-C system at 1073 K from THERMOCALC /17/.

- •targeted composition
- ■ S01
- • S04
- ✖ S06
- + S09 composition

Table 8

Normalized sample compositions

Sample ID	Temperature [K]	CH4 [Vol%]	C [mass%]	Ni [mass%]	W [mass%]
S01	1073	5	9.69	15.30	75.01
S02	1173	5	11.30	8.96	79.74
S03	1273	5	10.00	17.76	72.24
S04	1073	10	11.90	6.99	81.11
S05	1273	10	13.70	10.91	75.39
S06	1073	15	15.05	11.96	72.99
S07	1173	15	11.30	8.72	79.98
S08	1273	15	9.68	8.14	82.19
S09	1073	20	23.85	9.71	66.44

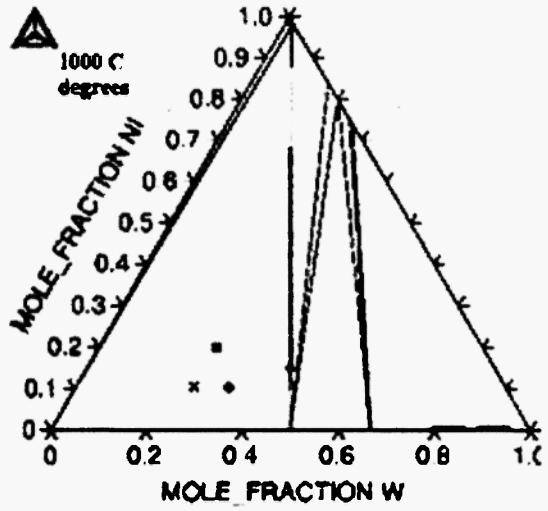

Fig. 14: The isothermal section of the Ni-W-C system at 1273 K from THERMOCALC /17/

•*targeted composition*

• *S03*

✖ *S05*

■ *S08*

The phase diagram corresponding to the highest temperature of the present investigation, *viz.*1273 K, extracted from THERMOCALC database is presented in **Figure 14**. This diagram does not differ significantly from that shown in Figure 13. The targeted composition as well as the sample compositions obtained (adopting the same procedure as at 1073 K, described above) are also plotted in the same figure.

Once again, the compositions of the samples synthesized are in the three phase region. This confirms the soundness of the present approach that the tailoring of the composition of the composite cemented carbide can be achieved by fine-tuning the gas composition, thus providing an excellent tool for process control.

The fugacities of the various species in the gas mixture and the corresponding activities of carbon in the solid state were computed from the FACT SAGE database. The results corresponding to 1073 K and the gas mixture 5 vol % CH_4 and 45 vol % H_2 (50 vol % Ar) are presented in the Appendix. The results of this computation were cross-checked using the Thermo-calc database. Both the results were in agreement with each other. It is seen in the Appendix that, for the above gas mixture, the activity of carbon in the solid phase is 1 with pure graphite as the standard state. The results for the other gas mixtures at the experimental temperatures were very similar indicating that the solid surface in contact with the gas mixture during the experiments will have solid carbon precipitated from the gas mixture. The amount of carbon precipitated will increase with increase in the CH_4 amount in the gas mixture. The carbon at the surface will diffuse into the bulk of the extremely fine alloy particles. That this diffusion process was fast at the experimental temperatures is evidenced by the uniformity of the product formed. In all the cases, XRD and bulk carbon analysis results show that the final product ended up in the WC-Ni-C three phase region. Further, the fraction of elemental carbon is found to increase with increasing amount of CH_4 in the gas mixture. This suggests that, at the end of the reduction process, the solid product is likely to be close to thermodynamic equilibrium with the gas phase and that, the gas mixture had reached the equilibrium state in the gas phase despite the fact that the temperatures used in the present experiments were slightly lower than those employed usually in equilibration with gas mixtures, *viz.* 1373 K and higher.

Another important aspect in the present investigation is the impact of temperature. It has been mentioned in the introduction part that grain size reduction during the synthesis would be extremely beneficial towards improved properties of the cemented carbide produced. Despite the fact that the fluidization technique would prevent, to a great extent, inter-particle contact, thereby minimizing the agglomeration of the particles, temperature is still an important factor in grain growth. In order to examine this, the average grain sized measured for the various samples are plotted as a function of the temperature of synthesis in **Figure 15**.

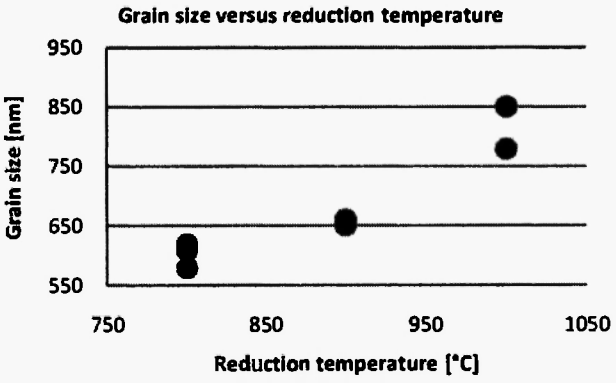

Fig. 15: Grain size versus reduction temperature

It is seen that the average grain size increases with increasing temperature indicating a high level of agglomeration at higher temperatures. It is to be noted that the value corresponding to the sample S06 was not considered in Figure 15 in view of the uncertainties in the grain size evaluation in the somewhat blurred SEM image. The sample S09 has also not been included due to the large amount of free carbon present leading to large deviation from targeted composition making a comparison with other samples untenable.

The significance of the present work is that the gas-solid reaction route is very promising with respect to the synthesis of cemented carbides of tailored composition. The present results also highlight the advantages of the application of the fluidized bed concept towards the synthesis of cemented carbides as this technique has the advantage of resulting in a product of uniform composition keeping at the same time the particles apart, thereby minimizing the agglomeration of particles due to solid-solid contacts. It is admitted that it would be desirable to achieve a further reduction in the particle size so that it could be in the nanometer range. The major obstacle in this context is the slow rate of the reduction-carburization reaction at 973 K as shown in the preliminary experiments. It is necessary to have knowledge of the kinetics of this reaction and understand the mechanism of the same in order to optimize the process. Kinetic studies of the reduction-carburization reaction are currently in progress in the present laboratory and we expect to publish the results very soon.

5. CONCLUSION

In the present work, Ni-WC cemented carbides were produced by a gas-solid reaction method using the oxides of nickel and tungsten as precursors and H_2-CH_4-Ar gas mixture as the reduction-carburization agent. A fluidized bed reactor was used in order to enable this reaction. The investigations were conducted in the temperature range 1073 – 1273 K.

The results showed that the compositions of the products synthesized were in conformity with the phase diagram of the Ni-W-C system in the experimental temperature range and were also close to the composition targeted for industrial applications. The carbon content in the product could be increased by increasing the chemical potential of carbon in the gas phase (by decreasing the H_2/CH_4 ratio in the gas mixture). It was also found that the product had an average grain size of about 0.55 μm at 1073K, which increased with increase in the process temperature.

The present results indicate the suitability of the application of reduction-carburization route by gas solid reaction in a fluidized bed reactor for industrial reduction of cemented carbides with tailored compositions.

ACKNOWLEDGEMENTS

The authors thank Dr. Olle Grinder for fruitful discussions and Miss L. Wang for help with FACT SAGE and Thermo Calc computations. The authors would like to thank Professor Dr. Vijaya Agarwala of Indian Institute of Technology Roorkee, India and Dr. Joanna Karwan-Baczewska, AGH – University of Science and Technology, Krakow, Poland for their support. Partial financial support to this project from SIDA-MENA project (D. no. 348-2006-6691) is also gratefully acknowledged.

7. REFERENCES

1. K. Schroter, US Pat., No. 1549615 (1925).
2. W. D. Schubert, H. Neumeister, G. Kinger and B. Lux, *Int. J. Refract. Met. Hard Mater.* **16**, No 2, 133-142 (1998).
3. Z. Yao, J. Jacob, A. Stiglich and T. S. Sudarshan, *Mater. Modif. Inc.*, **27**, 1 - 29 (1997).
4. M. Bahgat, M. K. Paek and J. J. Pak, *J. Alloys Compd.* **466**, No 2, 59-66 (2008).
5. H. Oswald, P. Kuhn and A. Reller, *Solid State Ion.* **32/33,** P 1, 528-536(1989).
6. C. Adorjan, A. Bock, S. Myllymaki, W.D. Schubert and K. Kontturi, *Int. J. Refract. Met. Hard Mater.* **26,** No.6, 569-574 (2008).
7. F. C. Alonso, M.L. Morales, A.U. Salas and J.E. Becerril, *Int. J. of Mineral Processing,* **20** , 137-151(1987).
8. D. S. Venables and M. E. Brown, *Thermochimica*

Acta, **291**, No.1, 131-140 (1997).
9. O. Ostrovski, and G. Zhang, *AlChE J.,* **52,** No. 1, 300- 310 (2005).
10. www.inframat.com/wcdetail.htm
11. A. Löfberg, A. Lrennet, G. Leclerq, L. Leclerq and J.M Giraudon, *J. Catal.* **189**, 170-183 (2000).
12. M. Boudart, S. T. Oyama, and L. Volpe, U.S. pat. 4,515,763 (1982).
13. L. Volpe and M. Boudart, *J. Solid State Chem.,* **59**, 348 - 356 (1985).
14. J. S. Lee, L. Volpe, F. H. Riberto, and M. Boudart, *J. Catal,* **112** ,44-53 (1988).
15. L. Volpe and M. Boudart, *Catal. Rev. Sci. Eng.,* **27** ,515 - 538(1985).
16. L. Volpe, L. Oyama, and M. Boudart, *Preparation of Catalysts III* edited by G. Poncelet, P. Grange and P.A. Jacobs, Elsevier, Amsterdam, (1983), pp. 147. 17 www.thermocalc.com/Products/TCW.html

APPENDIX

T = 1073.00 K
P = 1.00000E+00 atm
V = 9.13890E+03 dm3

STREAM CONSTITUENTS	AMOUNT/mol
H2	4.5000E+01
CH4	5.0000E+00
Ar	5.0000E+01

		EQUIL AMOUNT MOLE FRACTION		FUGACITY
PHASE:		**gas real**	**mol**	**atm**
H2		5.2527E+01	5.0622E-01	5.0637E-01
Ar		5.0000E+01	4.8186E-01	4.8200E-01
CH4		1.2363E+00	1.1915E-02	1.1919E-02
C2H4		2.2022E-05	2.1223E-07	2.1232E-07
C2H6	*T	2.1978E-06	2.1181E-08	2.1190E-08
H		1.0279E-06	9.9059E-09	9.9086E-09
CH3		5.1961E-07	5.0076E-09	5.0090E-09
C2H2		4.5346E-07	4.3702E-09	4.3718E-09
C2H3		2.9693E-12	2.8616E-14	2.8624E-14
CH2		5.7048E-15	5.4979E-17	5.4994E-17
C2H		2.9196E-15	2.8137E-17	2.8145E-17
CH		6.6549E-22	6.4135E-24	6.4153E-24
C		1.9403E-25	1.8699E-27	1.8704E-27
C3		3.1434E-27	3.0294E-29	3.0302E-29
C2		2.2714E-29	2.1890E-31	2.1896E-31
C5		5.1362E-35	4.9499E-37	4.9512E-37
C4		4.5124E-35	4.3487E-37	4.3499E-37
TOTAL:		1.0376E+02	1.0000E+00	1.0000E+00

	mol	**ACTIVITY**
C_graphite(s)	3.7636E+00	1.0000E+00
C_diamond(s2)	0.0000E+00	5.0123E-01

Cp_EQUIL	H_EQUIL	S_EQUIL	G_EQUIL	V_EQUIL
(J.K-1)	(J)	(J.K-1)	(J)	(dm3)
2.81519E+03	2.01975E+06	1.89616E+04	-1.83261E+07	9.13890E+03

Mole fraction of system components:

	gas real
Ar	3.1010E-01
C	7.6680E-03
H	6.8223E-01

Data on 1 constituent marked with '*T' are extrapolated outside their valid temperature range.